A Viologen Polymer and a Compact Ferrocene: Comparison of Solution Viscosities and Their Performance in a Redox Flow Battery with a Size Exclusion Membrane

*Philipp S. Borchers, Johannes Elbert, Ilya Anufriev, Maria Strumpf, Ivo Nischang, Martin D. Hager, and Ulrich S. Schubert**

In this work, the synthesis and characterization of a compact, ferrocene tetramer and a linear viologen polymer is reported. The latter material is a new, 4,4′-bipyridine containing, organo-soluble polymer. As aimed for solubility in nonpolar solvents, a 2-ethylhexyl-moiety to promote organosolubility and 4-vinylbenzyl serving as a polymerizable group are introduced to a 4,4′-bipyridine. The halide anions of the monomer cation are exchanged to bis(trifluoromethansulfon)imide, which further enhances organosolubility. The monomer is subsequently copolymerized with styrene by free radical polymerization. In addition, a four-ferrocene-containing compact structure, based on pentaerythritol, is synthesized via the straightforward radical thiol-ene reaction. The polymer solutions are thoroughly characterized hydrodynamically. Subsequently, propylene carbonate-based solutions of both materials are prepared to allow an assessment for future energy storage applications. This is done by testing battery characteristics in a custom-made flow-cell with a simple dialysis membrane for physical separation of the active materials. The capability of energy storage is verified by leaving the charged materials in solution in an open circuit for 24 h. Here, more than 99% of the stored charges can be recovered. Cycling the battery for 100 times reveals the remarkable stability of the materials of only 0.2% capacity loss per day in the battery setup.

1. Introduction

To overcome many hurdles of the energy transition from fossil fuels to renewable energies, redox flow batteries (RFBs) represent a promising solution.[1] The main hindrance of the implementation of renewable energies is their unpredictable energy output in terms of power and availability.[2] RFBs can help to overcome these challenges by storing overproduction of renewable energy sources, thus preventing voltage and frequency fluctuations, and providing electrical energy when the conditions for the generation of renewable energies are not met, for example, during night in case of solar energy harvesting. They thus provide a smooth electricity output for these otherwise unreliable energy platforms.[3] Because RFBs are driven by low cost and environmentally tolerable, that is, degradable materials and can scale energy and power independently, they can be used from a scale to support households up to industrial facilities.[4] In addition, the concepts and materials first pioneered for RFBs have recently led to new desalination and separation technologies.[5,6] Many materials,

P. S. Borchers, J. Elbert[+], I. Anufriev, M. Strumpf, I. Nischang, M. D. Hager, U. S. Schubert
Laboratory of Organic and Macromolecular Chemistry (IOMC)
Friedrich Schiller
University Jena
Humboldtstraße 10, 07743 Jena, Germany
E-mail: ulrich.schubert@uni-jena.de

P. S. Borchers, J. Elbert[+], M. Strumpf, M. D. Hager, U. S. Schubert
Center for Energy and Environmental Chemistry Jena (CEEC Jena)
Friedrich Schiller
University Jena
Philosophenweg 7a, 07743 Jena, Germany
I. Nischang, M. D. Hager, U. S. Schubert
Jena Center for Soft Matter (JCSM)
Friedrich Schiller
University Jena
Philosophenweg 7, 07743 Jena, Germany

The ORCID identification number(s) for the author(s) of this article can be found under https://doi.org/10.1002/macp.202100373

[+]Present address: Department of Chemical and Biomolecular Engineering, University of Illinois at Urbana-Champaign, Urbana, IL 61801, USA

ADVANCED
SCIENCE NEWS
www.advancedsciencenews.com

Macro-
molecular
Chemistry and Physics
www.mcp-journal.de

inorganic and organic, have been investigated for RFBs.[7] Heavy metals, however, raise concerns about long term environmental impacts and bear possible health-hazards.[8] Lately, organic molecules moved into the focus of researchers worldwide.[9] Organic molecules are advantageous in numerous ways. They are potentially cheaper compared to metals, even though they might need to be replaced more frequently. The lower price of organic materials, unlike, metals such as vanadium, originates from the absence of an established market, for example, the steel industry (ferrovanadium) for vanadium.[4,10] RFBs with organic active materials feature various different molecular classes, for example, tetramethylpiperidine-N-oxide (TEMPO),[11] phenothiazines,[12] quinones,[13] 4,4'-bipyridines,[14] and many more, with the active materials in either a monomeric or polymeric form.[15–18] Ferrocene plays an exceptional role in the list of active materials as it is long known for its extraordinary electrochemical stability[19] in both states of charge. It has successfully been applied in various RFBs under different conditions, for example, as a small molecule in aqueous batteries,[20,21] pendant on a polymer in organic batteries with a size exclusion separation membrane,[22] and pendant on a polymer in aqueous batteries with a size exclusion separation membrane.[23] Applying redox-active polymers as well as oligomers as active materials in RFBs is common practice nowadays,[1,16,24,25] as it has the advantage of requiring comparably cheap size exclusion membranes for physical separation of the charge carriers. A major drawback of using polymers as an active material in RFBs can be associated to a higher viscosity of the polymer-containing solutions when compared to small molecules, particularly at the high concentrations required for achieving sufficient energy densities. High viscosities lead to very high power demands for pumping the solutions, which may even exceed the power of the cell.[26,27] Polymer-based flow batteries make use of simple size exclusion membranes from regenerated cellulose (RC) materials, which are stable throughout a wide range of solvents, offer good size-based separation properties, and are comparably cheap. They have successfully been used for aqueous[18] and non-aqueous[22] RFBs.

In this contribution, we examine the feasibility and the viscosity advantages of cycling a new organosoluble polyviologen versus a straightforward to synthesize thio-ether linked, compact ferrocene from commercially available materials in an all organic RFB with a size exclusion membrane. For this purpose, we synthesized a compact, ferrocene-containing structure from penthaerythritol by attaching four redox-active ferrocene units to it, serving as a core for the compact molecule.[28] A similar molecule was already used in a RFB and showed good cycling behavior against a perylene.[29] However, with upscaling in mind, the reported etherification procedure for the ferrocene-containing molecule was not followed, as it involved precarious reagents such as the highly corrosive aluminum chloride and various metal hydrides. Furthermore, perylenes are prone to π-stacking and, thus, often come with the disadvantage of very low solubility.[30] As a consequence, a new organosoluble polymer with the well-established 4,4'-bipyridine was synthesized as active material, as it circumvents many of the aforementioned issues.

Viologen polymers have been successfully used in aqueous[31] as well as organic[22] battery systems. By using styrene as the comonomer, 2-ethylhexyl side chains as solubility-promoting
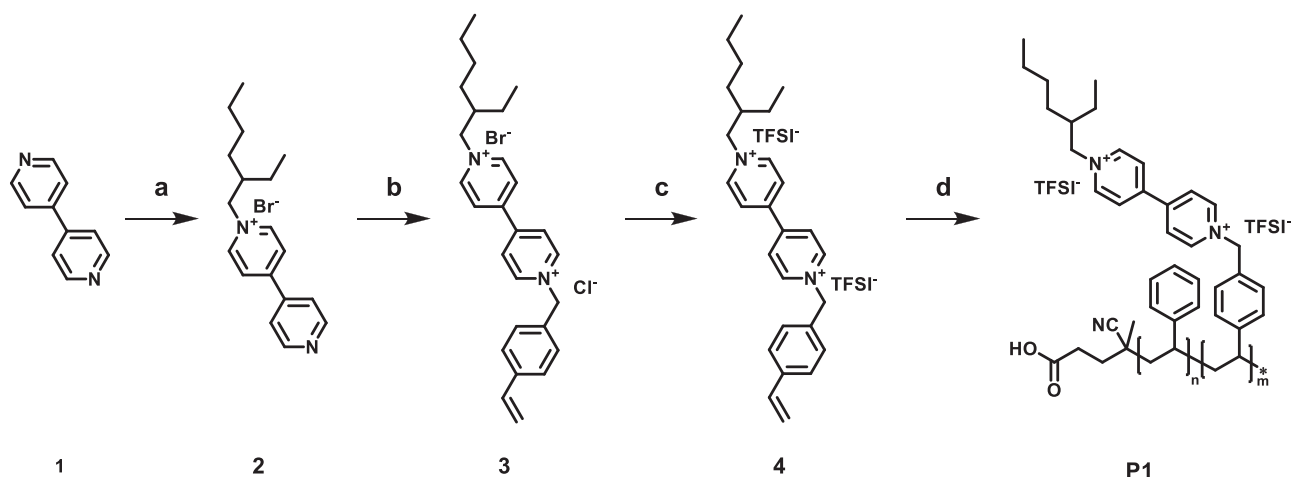
moieties and bis(trifluoromethansulfon)imide as the counterions, the polymer was tailored for the used battery setup. The materials in solution were electrochemically characterized and tested in a custom-made flow-cell. The battery showed charge storage for one day with high recovery rates exceeding 99%. Furthermore, the system underwent more than 100 charge- and discharge-cycles with only minor apparent capacity losses, revealing the stability in perspective of future applications of viologen polymers and compact ferrocene-containing structures in organic RFBs. Finally, the solution viscosities under battery setup conditions were compared, outlining an advantage of the compact ferrocene moiety containing structure as opposed to the viologen-containing linear polymer.

2. Results and Discussion

2.1. Synthesis of the Active Materials

The target was to examine the feasibility of using a polymeric material in a convenient and cost-efficient size exclusion membrane setup,[18] together with a compact, yet non-polymeric charge carrier and its advantages, that is, foremost the reduction of solution viscosity but also the appreciably enhanced diffusion and the favorable charge to mass ratio.[20] For this purpose, molecules that show a high stability in both, their charged and non-charged state are desired. Those should be readily soluble in the desired solvent, have a favorable charge to mass ratio and be conveniently synthesizable for future upscaling-projects. Beside the aforementioned properties, we also needed the tailor-made ferrocene to be retained by a size exclusion membrane. Therefore, a compact molecule, yet of a relatively high molar mass of ≥ 1000 g mol^{-1}, was aimed at, such that the charge carrier can still be retained by commercially available size exclusion membranes. The membranes in this separation range are usually made out of cellulose acetate or RC, with the second being very stable in most solvents applied in organic RFBs.

As material with a negative electrochemical potential in respect to ferrocene, 4,4'-bipyridine shows desirable properties, that is, it has proven to be exceptionally stable in the charged state when kept in an oxygen free atmosphere. It has already been used as a small molecule in water,[14] as a water-soluble polymer,[18] and as an organo-soluble polymer[22] for energy storage applications. In our case, a viologen that is readily organosoluble is needed. Commonly, at least one alkyl chain is attached to the bipyridine while the halide can be exchanged with tetrafluoroborate.[22,32] To facilitate the organosolubility, we attached a 2-ethylhexyl group (**Scheme 1**) to the 4,4'-bipyridine and used bis(trifluoromethanesulfon)imide (TFSI) as counterion. TFSI$^-$ and BF$_4^-$ are known as good promotors of organosolubility[33,34] and the TFSI ion is electrochemically stable in the desired voltage range. Tetrafluoroborate, on the other hand, is known to be a source of fluorine in numerous reactions,[35] thus bearing possible problems for the long term stability in battery systems. A styrene-type moiety was introduced by reaction with 4-chloromethylstyrene to allow polymerization and create the perspective active material. Styrene was used as a comonomer in the polymerization to further promote organosolubility of the resultant polymer in all states of charge. Adding soluble comonomers was successfully used in previous works, see,

ADVANCED
SCIENCE NEWS
www.advancedsciencenews.com

[M]acro-molecular
Chemistry and Physics
www.mcp-journal.de

Scheme 1. Schematic representation of the synthesis of the viologen polymer. a) 2-Ethylhexylbromide, NaI, CH_3CN, 24 h reflux. b) 4-Chloromethylstyrene, CH_3CN, 24 h reflux. c) LiTFSI, H_2O/ethyl acetate (EtOAc), 24 h room temperature. d) Styrene, 4,4′-azobis(4-cyanovaleric acid) (ACVA, 6 mol%), ethanol, 24 h 80 °C. * resembles any group suitable for quenching the radical polymerization.
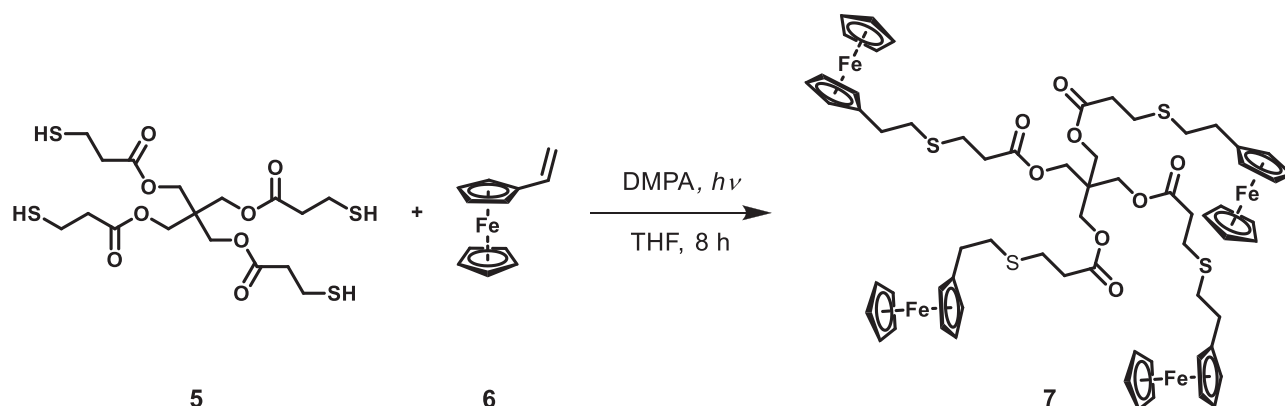
for example, Janoschka et al.[18] Due to the styryl moiety in the bipyridine monomer, one can expect copolymerization in a statistical manner. Free radical polymerization was chosen as polymerization technique because it is robust, tolerates a wide range of monomers, and works under rather mild conditions.

The polymerization of the bipyridine moiety achieved a satisfying conversion of above 90% after 24 h, as evident from proton nuclear magnetic resonance (^{1}H NMR) with N,N-dimethylformamide (DMF) as the internal standard. After heating, the reaction solution appeared in a very dark purple color, which would eventually turn red when the vial was opened and the solution was exposed to oxygen from ambient air. The typical color without oxygen, which can also be found while using bipyridine in a battery setup, indicated electron uptake of the bipyridine. It may function as a regulator of the polymerization, where it captures electrons from radicals and eventually releases them, thus allowing further polymerization. A similar process is well known for the radical polymerization of vinyl ferrocene.[36]

Evaluation of the ^{1}H NMR signals of the reaction solution at the start of the polymerization shows a ratio of 1 (DMF, signal at $\delta \approx 8$ parts per million (ppm), equals 2.3 mmol) to 2.1 (bipyridine, signal at $\delta \approx 8.6$ ppm, target: 4.8 mmol) whereas the molar ratio should be 1 to 2.1. Comparison of the same signal from the DMF standard with the styrene signal (signal at $\delta \approx 7.5$ to 7.2 ppm, target: 4.8 mmol) shows a ratio of 1 to 2.1, with a targeted ratio of 2.1. The initially targeted monomer ratio of 1:1 was closely met, as evident by these data. Evaluation of the conversion can only be roughly performed, as the usable double bond protons between $\delta = 5.5$ ppm and $\delta = 5.0$ ppm are very close to the signal of water. The integral of the double bond protons of the bipyridine monomer ($\delta \approx 5.35$ ppm) indicates 2.48 (2 + water signal) protons, the integral of the double bond protons of the pure styrene ($\delta \approx 5.20$ ppm) shows 3.09 (2 + water signal) protons. The ratio should be 2:2, as confirmed by the previous signal examination. After 24 h reaction time, the integrals of the proton signals at the very same shifts are 0.23 and 0.74 protons, respectively. That indicates a conversion of 92% of the bipyridine monomer and a conversion of 78% of the styrene. After polymerization, the viologen polymer was dialyzed against a RC membrane (molecular weight cutoff (MWCO) 1 kDa), which ensured that only larger polymer chains are used for battery experiments.

In the ^{1}H NMR spectrum of the final polymer (Figure S10, Supporting Information), the ratio of the bipyridine signals and styrene signals is 8 to 8.19. Assuming that four of the protons in the styrene region originate from the bipyridine monomer, the remaining signal consists of 4.19 protons. This is 83% of the five protons that styrene should have in this region. This leads to a ratio of both comonomers of 1 bipyridine to 0.83 styrene. When comparing the conversion, styrene has roughly 85% of the bipyridine conversion, which provides additional evidence for this polymer composition. With this evaluation, one gram of the polymer contains 0.97 mmol viologen, which, assuming one electron stored per active unit, equals ≈26 milliampere hours (mAh) per gram of active material. Studies also indicate that two-electron storage can be realized under certain conditions, possibly doubling the capacity per mass.[37] The polymer (51 mg) was soluble in propylene carbonate (100 µL) at 50 °C (i.e., a concentration of 510 mg mL^{-1}). This quite high concentration for polymers enables theoretical solution concentrations of 13 Ah L^{-1} in terms of capacity. Lower molar masses would cause lower solution viscosities at the same capacity per gram of active material. However, too small molar masses could compromise the size exclusion separation of the active materials. Notably, quite some mass of the viologen concerns the TFSI ($M_{TFSI} \approx 280$ g mol^{-1}) counterion. Only 40% of the monomer's mass originates from the viologen and 60% of its weight from the associated TFSI. Further improvements in the capacity per mass could be expected by applying a homopolymer from 4. Also, there would still be room for significant charge per weight improvements by replacing the counterion, if such were desired. Exemplary, a viologen-modified polypyrrole was reported to have a theoretical capacity of 68 mAh g^{-1}.[38] A similar theoretical capacity of ≈60 mAh g^{-1} can be deduced from the structure of a water-soluble viologen-modified styrene acrylamide copolymer.[39] However, both of these polymers are for aqueous applications and use chloride as the lightweight counterion, which has only 13% of

**ADVANCED
SCIENCE NEWS**
www.advancedsciencenews.com

**[M] acro-
molecular**
Chemistry and Physics
www.mcp-journal.de

Scheme 2. Schematic representation of the synthesis of the ferrocene-containing redoxactive material, adapted from the literature.[28]

the TFSI's mass. For a perspective, a boron-dipyrromethene-containing polymer exhibited a specific capacity of 15 mAh g^{-1}.[40]

To enable separation of the molecules in an electrochemical application with a size-exclusion membrane, the ferrocene-derivate should have a large enough overall size. To achieve this, pentaerythritol was used as the base structure for the synthesis. The tetra-ester with 3-mercaptopropanoic acid is commercially available and already offers two important features, one being a spacer to allow for attachment of multiple ferrocene moieties on one central core unit, and the other being a thiol as a functional group for the ferrocene attachment. The use of commercially available vinylferrocene enabled modification of the core structure via the well-established radical thiol-ene reaction, as reported in the literature (**Scheme 2**).[28]

Even though an excess of vinylferrocene was used for the synthesis, the main problem remained incomplete functionalization of the tetra-thiol, which was mediated by a prolonged reaction time. The ferrocene was partially oxidized during this procedure, as could be seen by the green color of the crude product. This may further contribute to the incomplete functionalization, as the oxidation may be caused by electronegative radical species (i.e., sulfur-radicals)[41] being reduced by the ferrocene moiety. The multiple ferrocene moiety containing compact structure can store four electrons per molecular entity or 80.3 mAh per gram of material.

2.2. Characterization of the Active Materials for Electrochemical Applications

Cyclic voltammetry of the bipyridine polymer (Figure S14, Supporting Information) revealed a highly symmetric cycling behavior with the first reduction at −0.77 V and the second reduction taking place at −1.25 V. The corresponding oxidations took place at −1.10 and −0.63 V, respectively. The peak split of more than 59 mV indicated a quasi-reversible redox reaction behavior. The ferrocene of this compact structure (Figure S15, Supporting Information) was oxidized at 0.03 V and reduced at −0.07 V, which also hinted toward a quasi-reversible redox behavior, referenced against an Ag/AgNO$_3$ electrode. From cyclic voltammetry this resulted in a charge voltage (peak to peak) of 0.8 V and a discharge voltage (peak to peak) of 0.66 V, which appeared reasonable con-

cerning the actual voltages of 0.71 and 0.61 V that were found when cycling the battery at a current of ±10 mA (Figure S21, Supporting Information).

The solution viscosities of the active materials were assessed at a temperature of 25 °C. Initially, the density of pure propylene carbonate was measured to be 1.1994 g cm^{-3}, which is close to the literature value of 1.1992 g cm^{-3}.[42] Next, to assess the impact of the addition of the active material to the electrolyte, the densities of the solution of 7 and P1 were measured at the same concentrations as in the battery setup, that is, 621 mg of P1 (≈0.60 mmol viologen) and 503 mg of 7 (0.38 mmol 7, 1.5 mmol ferrocene) in each 15 mL propylene carbonate. The densities were 1.2623 and 1.2685 g cm^{-3}, respectively. Afterward, the viscosities of the same electrolyte solutions were evaluated and found to be 2.50 mPa s for pure propylene carbonate, 4.94 mPa s for 7 and 5.91 mPa s for P1 in propylene carbonate, respectively. Even though the concentration of the ferrocene-containing compact structure as the electroactive material was 2.5 times as high as the concentration of the viologen polymer, its viscosity was significantly lower, affirming that non-polymeric, and compact active materials, yet of reasonable size, are definitely advantageous when compared to linear polymers from a viscometric point of view.

To put this in a perspective, having a concentration of ≈32 mmol per kg of total electrolyte, we measured a viscosity of 5.91 millipascal seconds (mPa s) for P1 in solution. A structurally similar polymer was reported to form a solution from 0.32 mol kg^{-1} of the polymer and 0.32 mol kg^{-1} LiBF$_4$ in acetonitrile with a viscosity of 5.39 mPa s.[43] The slightly higher overall viscosity from the present study stems primarily from the higher viscosity of propylene carbonate in comparison to acetonitrile. It can be anticipated that lower molar mass polymers lead to lower solution viscosities. One just has to keep in mind the molar mass dependent size exclusion properties of the membrane allowing to separate the active materials.

A study by Zhang et al. presents solution characteristics of small molecules in battery electrolytes with viscosities ranging between 0.5 mPa s^{-1} and ≈3 mPa s^{-1}.[44]

Size exclusion chromatography of the polymer derived from free-radical polymerization appeared not feasible. A brief study via sedimentation velocity analytical ultracentrifugation (Figure S23, Supporting Information) in the solvent methanol indicated rather low average molar masses accompanied by a
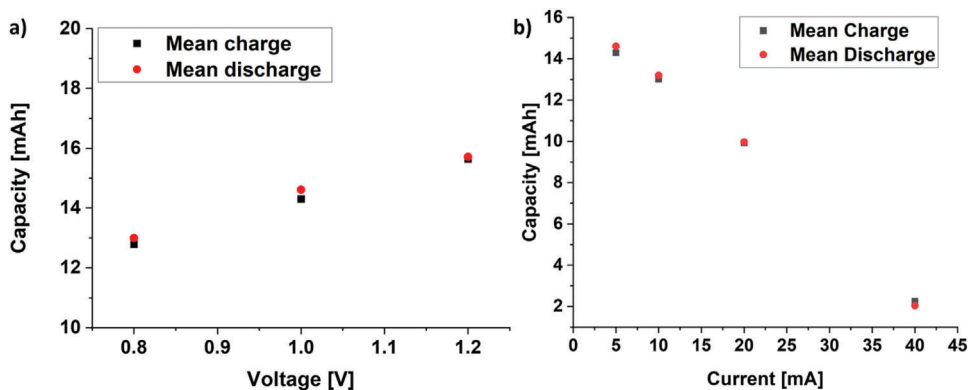
**ADVANCED
SCIENCE NEWS**

www.advancedsciencenews.com

Macro-
olecular
Chemistry and Physics

www.mcp-journal.de

Figure 1. a) Voltage dependent capacity at ±5 mA current and b) current dependent capacity at 1 V upper charge limit of the propylene carbonate-based poly-viologen and ferrocene RFB.

readily broad distribution as expected from the poor control of the free-radical polymerization process. The apparent molar masses averaged to ≈18.000 ($M_{s,f}$) and 24.000 g mol^{-1} ($M_{s,f}$) in the absence and presence of the salt, respectively (Table S1, Supporting Information). While the TFSI-salt of the monomer is highly hydrophobic, additional salt in the methanol might alter the polymer properties in solution, thus leading to a different apparent molar mass. In the presence of the LiTFSI, the apparent molar mass increased. The obtained molar mass values significantly exceed the exclusion limit of the utilized membrane.

Next, the material was tested in a custom-made flow battery, in which all tests were conducted with the same cell and the same material under an argon atmosphere. For testing, a battery with the polymer (P1) and the ferrocene-containing compact system (7) was assembled. In this case, the bipyridine was the capacity limiting side with a theoretical maximum charge capacity of ≈16.1 mAh, as calculated from the previously examined content of redox-active viologen per gram of polymer (vide supra). After equilibration of the cell and measuring the open circuit voltage (OCV, Figure S18, Supporting Information), the impedance was determined by potentio electrochemical impedance spectroscopy (PEIS, Figure S19, Supporting Information). It was found to be ≈7 Ω (35 Ω cm^2), being competitive with other all organic systems, comprising for example the ferrocene/bipyridine (363 Ω cm^2)[45] or the TEMPO/phthalimide (6.5 Ω cm^2).[46] The relatively low resistance, that is, for organic redox flow cells, demonstrates the feasibility of the RC membranes in the battery setup.[22]

As a first cycling test, the voltage dependent capacity was investigated. For this purpose, five charge discharge cycles were performed per voltage and the mean capacity over those cycles at 5 mA charging current was plotted (**Figure 1**a). A linear trend can be seen. However, as the bipyridine was the capacity-limiting component, the second reduction step already took place, as can be gauged from the second charge plateau in the voltage/time diagram (Figure S20, Supporting Information). To exclude the potentially irreversible reduction of the viologen, only the first reduction step was addressed. As a consequence, a maximum charging voltage of 1 V was chosen. In the second step, with the now fixed maximum charging voltage of 1 V and discharging voltage of 0.1 V, the response to different currents was tested (Figure 1b). The data were again averaged over five charge/discharge cycles for all currents. The measuring points from 5 mA charg-
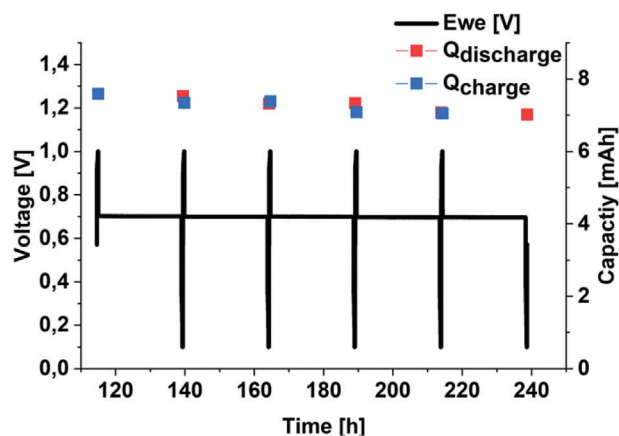

Figure 2. Test of the charge-storage capabilities of the battery by charging to 1 V with 20 mA, 5 min hold, 24 h rest, discharge with −20 mA to 0.1 V with 5 min hold. The test simulates a near-realistic use case for the RFB and demonstrates the stability of the used materials in their charged state.

ing current were taken from the previous test. Charging with 1.25 C of the theoretical capacity yielded ≈63% of the theoretical maximum charge. Charging with 2.5 C resulted in a charge value of ≈2 mAh or ≈12% of the maximum theoretically achievable value. For the given concentration and flow rate, which both play an important role when it comes to mass transport resistance considerations[47] and, hence, the maximum possible applicable charging and discharging currents, 10 mA charging current was found to provide sufficient cycling speed and observable capacity for cycling experiments. A current of 20 mA could, in this case, be considered a good rate for fast charging with a still considerable capacity. To put this into perspective, currents of 0.25 mA have also been reported for other polymer-based organic RFB.[40]

After examining the charge/discharge conditions for the cell-setup, the charge-storage capability of the material was investigated (**Figure 2**). For this purpose, the battery was charged with 20 mA to ≈50% of the theoretical maximum charge. This opened the possibility of destructive intermolecular interactions of charged and uncharged species, while providing a sufficient number of charged species to observe reactions with the solvent, the conducting salt or the membrane. After charging, the OCV
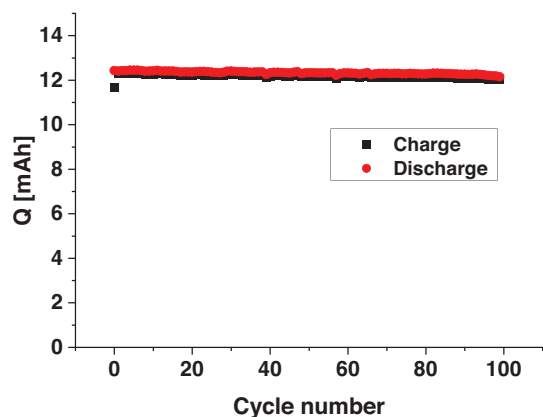
**ADVANCED
SCIENCE NEWS**

www.advancedsciencenews.com

**Macro-
molecular**
Chemistry and Physics

www.mcp-journal.de

Figure 3. Test of the long-term cyclability of the battery by charging to 1 V with 10 mA, 5 min hold, 5 min rest, discharge with −10 mA to 0.1 V. The test provides insight into the electrochemical stability of the materials and reveals absence of major side reactions during charging and discharging.

was measured and the charged solution was pumped through the cell for 24 h. No significant changes in the OCV could be observed during that period, indicating absence of undesirable reactions and self-discharge. During cycling, the overall charge capacity of the battery decreased from 7.59 to 7.05 mAh. An average of 99.5% of the charge could be extracted over five cycles, demonstrating good stability of the material in the charged state and a high charge recovery rate. The high recovery rate indicates no significant reaction of the charged molecule with the LiTFSI or the propylene carbonate and no decomposition of the molecule.

After demonstrating the promising properties of 7 and P1 for short term energy storage, the cyclability of the battery was investigated. Therefore, the battery was charged and discharged for 100 times (**Figure 3**) with 10 mA to 1 V maximum voltage. Thereon, it was further charged potentio-statically for five more minutes to ensure sufficient charge accumulation. Over 100 cycles, which ran over 11.1 days, the maximum charge capacity decreased from 12.31 mAh (first cycle with 11.69 mAh can be considered an outlier as the battery was not equilibrated) to 12.02 mAh. The discharge capacity decreased from 12.41 to 12.16 mAh. In other words, the charge capacity was reduced by 2.36%, which is 0.2% per day. The discharge capacity decreased by 2.02%, which is 0.18% per day. The overall higher discharge capacity might be explained by capacitor effects from previous experiments. In comparison, Montoto et al. reported a coulombic efficiency of more than 98% for a charge/discharge experiment over 50 cycles in an organic solvent,[22] while Milton et al. described their dendritic system to have a coulombic efficiency of >99.95% with a capacity retention of 99.994% per cycle.[48] To place our results further in perspective, Winsberg et al. reported a coulombic efficiency of >99.7% for a TEMPO-based system,[49] and >99% for a boron-dipyrromethene system.[40] Our results demonstrate the feasibility of a system comprising a polymer and a compact molecular structure containing four ferrocene moieties. They further highlight the appreciable charge storage capabilities and the cyclability of P1 and 7.

In contrast to the loss of ≈0.5 mAh over five days during the storage of the charged material, in this experiment just 0.3 mAh were lost throughout 11 days. This proofs that the loss during

the first experiment may not be caused by degradation of the active material, as a similar degradation rate should then be seen in the latter experiment as well. The reason for the capacity fade might be crossover of at least one of the active materials. After finishing the experiments, the electrolytes were subjected again to a CV measurement. The CV of the ferrocene-side (Figure S16, Supporting Information) revealed no noticeable signs of bipyridine-contamination. However, the CV spectrum of the bipyridine-polymer side (Figure S17, Supporting Information) clearly indicated signs of the presence of ferrocene moieties, pointing toward crossover of the ferrocene-containing compact structure through the membrane. To estimate the concentration of how much ferrocene 7 crossed the membrane, a concentration series of 7 at the exact same conditions was measured (Figure S22, Supporting Information). The base current was subtracted from the peak current and the results were plotted against the concentration. The results indicated, that the viologen-electrolyte, after all experiments, contained ≈1 mg mL^{-1} of 7. In other words, ≈15 mg of 7 crossed the membrane, which is ≈3% of the content of the ferrocene-electrolyte after three weeks of operation. The molar mass of 7 was ≈1337 g mol^{-1}, slightly above the specified MWCO of the membrane as specified for water with 90% retention of the active material.[50] However, in our battery setup the membranes pore size could be altered by using another solvent than water, affecting the MWCO.

Degradation of the active materials seemed to play no significant role, as no obvious changes, beside the ferrocene-crossover, could be seen in the CV of the battery-solutions after cycling the battery for three weeks overall. The marginal loss of capacity is well within the range of the determined crossover.

3. Conclusion

This initial study evaluated the combination of a four-ferrocene moiety containing, redox-active, and compact molecule versus a redox-active ferrocene-containing polymer for their feasibility in a RFB and highlighted the technological viscosity advantages of the compact ferrocene-containing structure. Therefore, we report the adapted synthesis of this ferrocene-containing structure[28] that served as the positive potential active material. It was paired with a new bipyridine-containing polystyrene, which was tailored in terms of solubility and stability for usage in organic RFB, and employed as negative potential active material. Both materials revealed highly stable quasi-reversible redox reactions in cyclic voltammetry. A battery was assembled, which revealed a resistance of 35 Ω cm^2, which is well within the range for typical organic RFB, allowing the battery to be (dis-)charged with 1.25 C over 100 cycles, where it lost ≈2.4% of its overall capacity. When charged, the charged solution was pumped through the battery for 24 h and more than 99% of the charge could still be extracted over five cycles. After battery testing, the solutions were again examined via cyclic voltammetry and revealed no crossover of the bipyridine polymer, but small amounts of the compact ferrocene moiety containing molecule. As could be seen from the battery experiments, the crossover appeared low by testing over three weeks of time, but should further be investigated within the context of upcoming studies. The size of the ferrocene-bearing molecule barely met the MWCO limit, rated for aqueous use in case of the RC membrane. Synthesis of larger structures,

involving the up-scalable thiol-ene chemistry, does not present a roadblock for larger scale devices.[51] Investigation of the viscosity of the battery solutions proved that compact structures with a multiplicity of ferrocene moieties have a much lower solution viscosity per active unit compared to linear polymer structures. Overall, tailored design of similar, yet larger structures, appears to be promising for future investigations, as they combine good charge to molar mass ratios with an overall lower contribution to solution viscosity, engineering-wise enabling more cost-efficient battery setups.

4. Experimental Section

Devices and Materials: All NMR spectra were recorded on Bruker Avance I 300 MHz and Bruker Avance III 400 MHz spectrometers.

Samples for elemental analysis were weighed with a Sartorius MC 5 and analyzed with a Euro EA 3000 from Heka Tech. The halogen content of samples was determined with a TLalpa20 titrator from siAnalytics.

Electrochemical tests were performed with a Bio Logic VSP 3 potentiostat.

Solution viscosity was measured with an AMVn microviscosimeter from Anton Paar.

A UV cube 100 with an iron bulb by Dr. Hönle AG was used to perform the thiol-ene click reaction.

Analytical ultracentrifugation was performed using a ProteomeLab XL-I analytical ultracentrifuge (Beckman Coulter Instruments, Brea, CA).

Synthesis of Ethylhexylbipyridinium Bromide 2: 4,4′-Bipyridine (31.7 g, 203 mmol) was dissolved in acetonitrile (250 mL). 2-Ethylhexylbromide (54 mL, 303 mmol) was added along with sodium iodide (2 g). The mixture was heated under gentle reflux for 24 h. Afterward, the hot suspension was filtered, and subsequently the solvent was removed from the filtrate. The orange residue was suspended in acetone with small quantities of methanol. The filtrate was then slowly given into a tenfold excess of diethyl ether. The precipitate was collected on a filter and repeatedly washed with diethyl ether, until no more 4,4′-bipyridine was visible in the NMR spectra. The solid was collected and dried to yield an orange powder (23.2 g, 66.4 mmol, 33%).

^{1}H NMR (300 MHz, CD$_3$OD, δ): 9.16–9.13 (d, 2 H, Pyr), 8.86–8.84 (dd, 2 H, Pyr), 8.58–8.56 (d, 2 H, Pyr-CH), 8.05–8.03 (dd, 2 H, Pyr), 4.66–4.64 (d, 2 H, N–CH$_2$), 2.17–2.09 (m, 1 H, CH), 1.53–1.34 (m, 8 H, CH$_2$), 1.02–0.96 (m, 6 H, CH$_3$).

Synthesis of N-Ethylhexyl-N′-(4-Vinyl)-Benzyl Bipyridinium Chloride Bromide 3: The bipyridine 2 (2 g, 5.73 mmol) was dissolved in acetonitrile (10 mL) and heated to 80 °C in a capped microwave vial. 4-Chloromethylstyrene (1.2 eq, 6.87 mmol, 0.97 mL) was added in one portion while the mixture was heated. Subsequently, the solution was heated for 24 h. The orange suspension was then filtered, and the solvent was removed from the filtrate. The resulting solid was washed with dichloromethane, until no more colored washing solution appeared. It was then dried on the filter, before being dried in vacuo. The product was received as orange powder (2.15 g, 75%).

^{1}H NMR (300 MHz, CD$_3$OD, δ): 9.40–9.30 (d, 2 H, Pyr), 9.33–9.30 (d, 2 H, Pyr), 8.76–8.72 (m, 4 H, Pry), 7.64–7.56 (m, 4 H, Ph), 6.83–6.74 (dd, 1 H, CH=CH$_2$), 6.02 (s, 2 H, Ph-CH$_2$), 5.91–5.85 (d, 1 H, CH=CH$_2$), 5.36–5.32 (d, 1 H, CH=CH$_2$), 4.74–4.71 (d, 2 H, Pyr-CH$_2$), 2.18–2.12 (m, 1 H, CH), 1.51–1.35 (m, 8 H, CH$_2$) 1.02–0.96 (m, 6 H, CH$_3$).

^{13}C NMR (75 MHz, CD$_3$OD, δ/ppm): 150.2, 149.9, 146.0, 145.6, 139.5, 135.7, 132.1, 129.5, 127.2, 127.0, 114.7, 65.2, 64.2, 41.2, 29.3, 27.9, 22.6, 22.5, 12.9, 9.1.

Synthesis of N-Ethylhexyl-N′-(4-Vinyl)-Benzyl Bipyridinium Di-Bistrifluoromethanesulfonamide 4: Bipyridine 3 (5.0 g, 3.985 mmol) was given into water (20 mL). Lithium bis(trifluoromethanesulfonyl)imide (LiTFSI, 2.5 eq, 7.15 g) was dissolved in water (5 mL). Ethyl acetate (EtOAc, 25 mL) was added to the solved bipyridine. The TFSI solution was added via a syringe. The mixture was vigorously stirred overnight.

Afterward, the biphasic solution was separated. The organic phase was diluted with EtOAc (50 mL) and washed with water (20 mL) containing LiTFSI (≈1 g). Afterward, the organic phase was washed with water (30 mL) containing ≈500 mg AgNO$_3$ and 1 g LiTFSI. Thereafter, the organic phase was washed with water, dried over Na$_2$SO$_4$, filtered, and the solvent was evaporated under reduced pressure. The product (9.4 g, ≈100%) was received as highly viscous and very sticky fluid.

^{1}H NMR (300 MHz, CD$_3$OD, δ): 9.25–9.22 (d, 2 H, Pyr-CH), 9.19–9.17 (d, 2 H, Pyr-CH), 8.64–8.60 (m, 4 H, Pry-CH), 7.58–7.52 (m, 4 H, Ph), 6.82–6.73 (dd, 1 H, CH=CH$_2$), 5.93 (s, 2 H, Ph-CH$_2$), 5.90–5.84 (dd, 1 H, CH=CH$_2$), 5.35–5.31 (dd, 1 H, CH=CH$_2$), 4.67–4.64 (d, 2 H, Pyr-CH$_2$), 2.16–2.09 (m, 1 H, CH), 1.49–1.33 (m, 8 H, CH$_2$) 1.00–0.90 (m, 6 H, CH$_3$).

^{13}C-NMR (300 MHz, CD$_3$OD, δ): 150.4, 150.1, 145.9, 145.5, 139.5, 135.7, 131.7, 129.4, 127.2, 127.1, 127.0, 126.1, 121.9, 65.3, 64.3, 53.4, 41.2, 29.3, 27.8, 22.6, 22.4, 12.9, 9.0.

Polymerization P1: All operations until dialysis were performed under argon.

The viologen monomer 4 (4.5 g, 4.75 mmol) was placed inside a microwave vial. Ethanol (8 mL) was added and the monomer was stirred until all material was dissolved. Meanwhile, argon was bubbled through the solution for ≈20 min. Styrene (≈3 mL) was extracted with NaOH (10% in water, ≈5 mL). The styrene-phase was separated and dried over Na$_2$SO$_4$. Afterward, it was passed over alkaline aluminum oxide. The colorless styrene (546 µL, 4.75 mmol) was transferred into the ethanol solution via an Eppendorf pipette. DMF (175 µL, 2.27 mmol) was added as internal standard. 4,4′-azobis(4-cyanovaleric acid) (ACVA, 80 wt%, 318 mg, 0.6 mmol, ≈6 mol%) was added at once, a NMR sample (50 µL in 600 µL CD$_3$OD, P1-0h) was taken and the vial was recapped and transferred to the microwave, where the yellowish solution was heated to 80 °C for 24 h. The next day, a dark-red solution was received, after the vial was left in the microwave (without heating) overnight. Another NMR sample (50 µL in 600 µL CD$_3$OD), P1-24h was prepared. The mixture was subsequently dialyzed in a dialysis tube (MWCO = 1 kDa, one day dialysis time) against ethanol, which showed little effect. Dialysis in a dialysis tube (MWCO = 1 kDa, two days dialysis time) against acetone resulted in a red dialysis solution, which was renewed once. Removal of the solvent from the solution inside the dialysis tube yielded the pure polymer (2.66 g, 53% of theor. mass).

^{1}H NMR (300 MHz, THF^{D8}, δ): 9.04 (s, 4 H, pyr), 8.50 (s, 4 H, Pyr), 7.50–6.16 (b, 8.23 H, styrene-monomers) 5.98–5. 80 (b, 1.84 H, styrene-Ph), 4.71–4.44 (b, 1.87 H, pyr-CH$_2$), 2.12–1.96 (b, CH), 1.47–1.21 (b, ethylhexyl + styrene backbone), 1.0–0.7 (m, CH$_3$)

Synthesis of Vinylferrocene 6: Similar to standard literature procedures,[52] methyltriphenylphosphonium bromide (47.3 g, 132 mmol) was dried in vacuo for 20 min. Dry tetrahydrofuran (THF) (600 mL) was added and the dispersion was cooled to −70 °C. n-BuLi (150 mmol, 60 mL in n-hexane) was slowly added and the mixture was stirred for 20 min at room temperature. Afterward, it was cooled to −70 °C again. Ferrocene carboxaldehyde (21 g, 98 mmol) was dissolved in dry THF (150 mL) and slowly added to the ylide. The mixture was stirred for 16 h while slowly warming to room temperature. Afterward, the mixture was filtrated and the solvent was removed in vacuo. The residue was dissolved in diethyl ether (500 mL) and washed with water and brine, before being dried over MgSO$_4$. Subsequently, the solvent was removed and the raw product was purified by column chromatography (stationary phase: SiO$_2$, mobile phase: n-hexane). The product (18.35 g, 88%) was obtained as orange powder. The analytical data matched those from the literature.[52]

Synthesis of Pentaerythritol Tetrakis(5-Ferrocene-3-Sulfahexanoate) 7: According to a literature procedure,[28] vinylferrocene was reacted with pentaerythritol tetrakis(3-mercaptopropionate) under UV light with 2,2-dimethoxy-2-phenylacetophenon (DMPA) as radical initiator. Two batches were prepared. For the first batch, vinylferrocene (5.0 g, 23.6 mmol) and pentaerythritol tetrakis(3-mercaptopropionate) (2.1 g, 4.3 mmol) and DMPA (0.11 g, 0.43 mmol, 2.5% resp. to thiol groups) were dissolved in THF (20 mL). The mixture was deoxygenated by bubbling through argon. Afterward, it was irradiated in a UV-cube for six times, each at 20 min. Between irradiation, the solution was cooled to ambient temperature to prevent the solvent from boiling. The solvent was removed in vacuo and

the residue was bound to silica, before being purified via column chromatography (n-hexane/ethyl acetate 70/30, $r_F = 0.44$). The product was obtained with impurities, that is, incompletely functionalized thiols, (1.6 g combined) and used for a subsequent photoreaction.

The second batch was prepared following the same procedure with the exact same amounts of reagents. Multiple purifications via column chromatography (same eluent mixture) yielded a pure product (0.8 g) and a mixture of product and byproduct (together $\approx$1.5 g), which was used for the same re-functionalization as the prior mixture. The described fractions of the mixed products ($\approx$3.1 g) from both earlier batches were united and, together with vinylferrocene (1.18 g, 5.56 mmol) and DMPA (71 mg, 0.29 mmol), dissolved in THF (10 mL), degassed, and irradiated as described above with 24 × 20 min irradiation time. Column chromatography was conducted as described above, yielding pure product (2.4 g, $\approx$1.80 mmol). Together with the first pure fraction, that is 2.4 mmol (28% in respect to the thiol). The analytical data were in good agreement with literature.[28]

^{1}H NMR (300 MHz, CDCl$_3$, δ/ppm): 4.18 (s, 2 H, OCH$_2$), 4.13 (s, 9 H, C$_5$H$_5$), 4.12–4.09 (d, 4 H, C$_5$H$_4$), 2.81–2.60 (m, 8 H, CH$_2$).

Anal. calcd for C$_{65}$H$_{75}$Fe$_4$O$_8$S$_4$ C 58.40 H 5.73, S 9.52; found: C 58.42 H 5.76, S: 9.52.

Analytical Ultracentrifugation: The bipyridine polymer was studied via sedimentation velocity analytical ultracentrifugation in pure methanol ($\rho_0 = 0.7913$ g cm^{-3}, $\eta_0 = 0.595$ mPa s) and in 0.1 M LiTFSI in methanol ($\rho_0 = 0.8111$ g cm^{-3}, $\eta_0 = 0.651$ mPa s) as solvents at $T = 20$ °C. The partial specific volume, υ, of the polymer was determined as described recently.[53]

For molar mass calculations, sedimentation velocity experiments were performed using a ProteomeLab XL-I analytical ultracentrifuge (Beckman Coulter Instruments, Brea, CA) with an An-50 Ti eight-hole rotor. Cells with double-sector aluminum centerpieces with a 12 mm optical solution path length were filled with 420 µL of polymer solution and 440 µL of the solvent in the reference sector. The measurements were carried out at a rotor speed of 42 000 rpm, a temperature of $T = 20$ °C, and in a concentration range of $0.05 \cdot 10^{-2}$ to $0.35 \cdot 10^{-2}$ g cm^{-3}. Analysis of experimental data was performed via the ls-g*(s) and c(s) models in SEDFIT.[54,55] Since no clear trend in the dependence of sedimentation coefficients, s, and translational frictional ratios, f/f_{sph}, from sedimentation-diffusion analysis was observed, their values were averaged over the utilized concentration range. The molar masses based on s and f/f_{sph} values were calculated according to the modified Svedberg equation.[53]

Battery Testing: For battery testing, the polymer P1 (621 mg, $\approx$0.59 mmol bipyridine) and the ferrocene tetramer 7 (503 mg, $\approx$1.51 mmol ferrocene) were each placed in a separate vial. Propylenecarbonate (each 15 mL) was added and argon was bubbled through the solution for 30 min. While deoxygenating, LiTFSI (2.87 g each, $\approx$0.67 M conducting salt) was added to each vial. The solutions were transferred to an argon glovebox. In there, they were pumped with a peristaltic pump through a custom-made battery cell. The cell consists of graphite electrodes and uses graphite felts in the flow chambers. RC membrane (MWCO = 1 kDa, CarlRoth) was used as separator of the two half cells.

Potentio Electrochemical Impedance Spectroscopy: E_{WE} was set to 0 V with reference to the OCV. The scanning range was from 1 MHz to 1 Hz with 12 points per decade and logarithmic point spacing. The sinus amplitude was 10 mV. A short rest time of 0.1 periods was set before each frequency and two measurements per frequency were performed. The E range was −2.5 to 2.5 V as device standard setting, resulting in a resolution of 100 µV. The measurement was done with the assembled cell stack, meaning the graphite plates and felts served as electrodes and the overall resistance of the setup was measured.

Quantification of the Ferrocene Content after Cell Cycling: The same setup and techniques that were used to measure the CV spectrum of the viologen-solution from the battery, were utilized to determine a concentration series of 7 in propylene carbonate with 0.67 M LiTFSI as conducting salt, that is, the same conditions as for the battery electrolyte. The stock solution was added to a solution (5 mL) of 0.67 M LiTFSI in propylene carbonate. After each aliquot, cyclic voltammetry was measured and the second cycle was plotted and used for evaluation (Figure S22, Supporting

Information). The base current was interpolated and subtracted from the peak current for all relevant voltammograms. A linear plot could be made from the data to estimate the content of 7 to $\approx$1 mg mL^{-1}.

Supporting Information

Supporting Information is available from the Wiley Online Library or from the author.

Conflict of Interest

The authors declare no conflict of interest.

Data Availability Statement

The data that support the findings of this study are available from the corresponding author upon reasonable request.

[1] J. Luo, B. Hu, M. Hu, Y. Zhao, T. L. Liu, *ACS Energy Lett.* **2019**, *4*, 2220.

[2] A. B. Gallo, J. R. Simões-Moreira, H. K. M. Costa, M. M. Santos, E. Moutinho Dos Santos, *Renewable Sustainable Energy Rev.* **2016**, *65*, 800.

[3] T. Shibata, T. Kumamoto, Y. Nagaoka, K. Kawase, K. Yano, *SEI Tech. Rev.* **2013**, *76*, 14.

[4] P. Alotto, M. Guarnieri, F. Moro, *Renewable Sustainable Energy Rev.* **2014**, *29*, 325.

[5] N. Kim, J. Jeon, J. Elbert, C. Kim, X. Su, *Chem. Eng. J.* **2022**, *428*, 131082.

[6] N. Kim, S. P. Hong, J. Lee, C. Kim, J. Yoon, *ACS Sustainable Chem. Eng.* **2019**, *7*, 16182.

[7] J. Ye, L. Xia, C. Wu, M. Ding, C. Jia, Q. Wang, *J. Phys. D: Appl. Phys.* **2019**, *52*, 443001.

[8] J. A. J. Watt, I. T. Burke, R. A. Edwards, H. M. Malcolm, W. M. Mayes, J. P. Olszewska, G. Pan, M. C. Graham, K. V. Heal, N. L. Rose, S. D. Turner, B. M. Spears, *Environ. Sci. Technol.* **2018**, *52*, 11973.

[9] J. Winsberg, T. Hagemann, T. Janoschka, M. D. Hager, U. S. Schubert, *Angew. Chem., Int. Ed.* **2017**, *56*, 686.

[10] F. R. Brushett, M. J. Aziz, K. E. Rodby, *ACS Energy Lett.* **2020**, *5*, 879.

[11] T. Suga, H. Konishi, H. Nishide, *Chem. Commun.* **2007**, 1730.

[12] N. H. Attanayake, J. A. Kowalski, K. V. Greco, M. D. Casselman, J. D. Milshtein, S. J. Chapman, S. R. Parkin, F. R. Brushett, S. A. Odom, *Chem. Mater.* **2019**, *31*, 4353.

[13] D. G. Kwabi, K. Lin, Y. Ji, E. F. Kerr, M.-A. Goulet, D. De Porcellinis, D. P. Tabor, D. A. Pollack, A. Aspuru-Guzik, R. G. Gordon, M. J. Aziz, *Joule* **2018**, *2*, 1894.

[14] T. Janoschka, N. Martin, M. D. Hager, U. S. Schubert, *Angew. Chem., Int. Ed.* **2016**, *55*, 14427.

[15] V. Singh, S. Kim, J. Kang, H. R. Byon, *Nano Res.* **2019**, *12*, 1988.

[16] Y. Y. Lai, X. Li, Y. Zhu, *ACS Appl. Polym. Mater.* **2020**, *2*, 113.

[17] S. Muench, A. Wild, C. Friebe, B. Häupler, T. Janoschka, U. S. Schubert, *Chem. Rev.* **2016**, *116*, 9438.

[18] T. Janoschka, N. Martin, U. Martin, C. Friebe, S. Morgenstern, H. Hiller, M. D. Hager, U. S. Schubert, *Nature* **2015**, *527*, 78.

[19] R. R. Gagne, C. A. Koval, G. C. Lisensky, *Inorg. Chem.* **1980**, *19*, 2854.

[20] E. S. Beh, D. De Porcellinis, R. L. Gracia, K. T. Xia, R. G. Gordon, M. J. Aziz, *ACS Energy Lett.* **2017**, *2*, 639.

[21] B. Hu, C. Debruler, Z. Rhodes, T. L. Liu, *J. Am. Chem. Soc.* **2017**, *139*, 1207.

[22] E. C. Montoto, G. Nagarjuna, J. S. Moore, J. Rodríguez-López, *J. Electrochem. Soc.* **2017**, *164*, A1688.

[23] P. S. Borchers, M. Strumpf, C. Friebe, I. Nischang, M. D. Hager, J. Elbert, U. S. Schubert, *Adv. Energy Mater.* **2020**, *10*, 2001825.

[24] S. Odom, *ACS Cent. Sci.* **2018**, *4*, 140.

[25] M. J. Baran, M. N. Braten, E. C. Montoto, Z. T. Gossage, L. Ma, E. Chénard, J. S. Moore, J. Rodríguez-López, B. A. Helms, B. A. Helms, *Chem. Mater.* **2018**, *30*, 3861.

[26] D. Takagi, N. J. Balmforth, *J. Fluid Mech.* **2011**, *672*, 196.

[27] J. D. Milshtein, R. M. Darling, J. Drake, M. L. Perry, F. R. Brushett, *J. Electrochem. Soc.* **2017**, *164*, A3883.

[28] I. Martínez-Montero, S. Bruña, A. M. González-Vadillo, I. Cuadrado, *Macromolecules* **2014**, *47*, 1301.

[29] M. Milton, Q. Cheng, Y. Yang, C. Nuckolls, R. Hernández Sánchez, T. J. Sisto, *Nano Lett.* **2017**, *17*, 7859.

[30] M. Sun, K. Müllen, M. Yin, *Chem. Soc. Rev.* **2016**, *45*, 1513.

[31] T. Janoschka, N. Martin, U. Martin, C. Friebe, S. Morgenstern, H. Hiller, M. D. Hager, U. S. Schubert, *Nature* **2015**, *527*, 78.

[32] C. Chen, S. Zhang, Y. Zhu, Y. Qian, Z. Niu, J. Ye, Y. Zhao, X. Zhang, *RSC Adv.* **2018**, *8*, 18762.

[33] V. Ho, B. W. Boudouris, R. A. Segalman, *Macromolecules* **2010**, *43*, 7895.

[34] R. Marcilla, J. Alberto Blazquez, J. Rodriguez, J. A. Pomposo, D. Mecerreyes, *J. Polym. Sci., Part A: Polym. Chem.* **2004**, *42*, 208.

[35] A. J. Cresswell, S. G. Davies, P. M. Roberts, J. E. Thomson, *Chem. Rev.* **2015**, *115*, 566.

[36] C. U. Pittman, *J. Inorg. Organomet. Polym. Mater.* **2005**, *15*, 33.

[37] C. Debruler, B. Hu, J. Moss, X. Liu, J. Luo, Y. Sun, T. L. Liu, *Chem* **2017**, *3*, 961.

[38] S. Sen, J. Saraidaridis, S. Y. Kim, G. T. R. Palmore, *ACS Appl. Mater. Interfaces* **2013**, *5*, 7825.

[39] T. Janoschka, S. Morgenstern, H. Hiller, C. Friebe, K. Wolkersdörfer, B. Häupler, M. D. Hager, U. S. Schubert, *Polym. Chem.* **2015**, *6*, 7801.

[40] J. Winsberg, T. Hagemann, S. Muench, C. Friebe, B. Häupler, T. Janoschka, S. Morgenstern, M. D. Hager, U. S. Schubert, *Chem. Mater.* **2016**, *28*, 3401.

[41] F. De Vleeschouwer, V. Van Speybroeck, M. Waroquier, P. Geerlings, F. De Proft, *Org. Lett.* **2007**, *9*, 2721.

[42] P. K. Muhuri, D. K. Hazra, *J. Chem. Eng. Data* **1994**, *39*, 375.

[43] V. A. Iyer, J. K. Schuh, E. C. Montoto, V. Pavan Nemani, S. Qian, G. Nagarjuna, J. Rodríguez-López, R. H. Ewoldt, K. C. Smith, *J. Power Sources* **2017**, *361*, 334.

[44] J. Zhang, R. E. Corman, J. K. Schuh, R. H. Ewoldt, I. A. Shkrob, L. Zhang, *J. Phys. Chem. C* **2018**, *122*, 8159.

[45] J. Chai, A. Lashgari, Z. Cao, C. K. Williams, X. Wang, J. Dong, J. J. Jiang, *ACS Appl. Mater. Interfaces* **2020**, *12*, 15262.

[46] J. Winsberg, S. Benndorf, A. Wild, M. D. Hager, U. S. Schubert, *Macromol. Chem. Phys.* **2018**, *219*, 1700267.

[47] D. Aaron, Z. Tang, A. B. Papandrew, T. A. Zawodzinski, *J. Appl. Electrochem.* **2011**, *41*, 1175.

[48] M. Milton, Q. Cheng, Y. Yang, C. Nuckolls, R. Hernández Sánchez, T. J. Sisto, *Nano Lett.* **2017**, *17*, 7859.

[49] J. Winsberg, T. Janoschka, S. Morgenstern, T. Hagemann, S. Muench, G. Hauffman, J.-F. Gohy, M. D. Hager, U. S. Schubert, *Adv. Mater.* **2016**, *28*, 2238.

[50] E. Drioli, C. A. Quist-Jensen, L. Giorno, in *Encyclopedia of Membranes* (Eds: E. Drioli, L. Giorno), Springer, Berlin **2016**, p. 1326.

[51] K. L. Killops, L. M. Campos, C. J. Hawker, *J. Am. Chem. Soc.* **2008**, *130*, 5062.

[52] M. I. R. Valderrama, R. A. V. García, T. Klimova, E. Klimova, L. Ortiz-Frade, M. M. García, *Inorg. Chim. Acta* **2008**, *361*, 1597.

[53] M. Grube, M. N. Leiske, U. S. Schubert, I. Nischang, *Macromolecules* **2018**, *51*, 1905.

[54] P. Schuck, P. Rossmanith, *Biopolymers* **2000**, *54*, 328.

[55] P. Schuck, *Biophys. J.* **2000**, *78*, 1606.